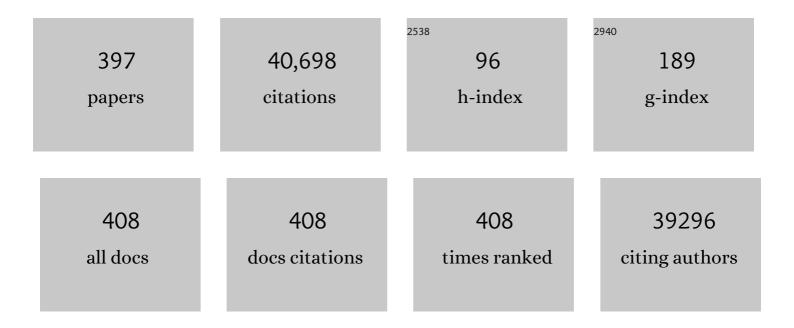
List of Publications by Year in descending order

Source: https://exaly.com/author-pdf/6108350/publications.pdf Version: 2024-02-01



SHUVAN SONG

#	Article	IF	CITATIONS
1	Cascade-responsive nanobomb with domino effect for anti-tumor synergistic therapies. National Science Review, 2022, 9, nwab139.	4.6	29
2	MOF/PCP-based Electrocatalysts for the Oxygen Reduction Reaction. Electrochemical Energy Reviews, 2022, 5, 32-81.	13.1	47
3	Increased solar absorption and promoted photocarrier separation in atomically thin 2D carbon nitride sheets for enhanced visible-light photocatalysis. Chemical Engineering Journal, 2022, 431, 133219.	6.6	7
4	A Bimetallic Nanozyme with Cascade Effect for Synergistic Therapy of Cancer. ChemMedChem, 2022, 17,	1.6	10
5	Bimetallic catalyst derived from copper cobalt carbonate hydroxides mediated ZIF-67 composite for efficient hydrogenation of 4-nitrophenol. Colloids and Surfaces A: Physicochemical and Engineering Aspects, 2022, 641, 128477.	2.3	8
6	Boosting the Catalytic Performance of CuO _x in CO ₂ Hydrogenation by Incorporating CeO ₂ Promoters. Advanced Sustainable Systems, 2022, 6, .	2.7	6
7	Self-Assembled Nanocomposites and Nanostructures for Environmental and Energy Applications. Crystals, 2022, 12, 274.	1.0	0
8	Dualâ€Site Singleâ€Atom Catalysts with High Performance for Threeâ€Way Catalysis. Advanced Materials, 2022, 34, e2201859.	11.1	39
9	Modulation of the Host–Guest–Guest Interactions in a Metal–Organic Framework for Multiple Anticounterfeiting Applications. Inorganic Chemistry, 2022, 61, 456-463.	1.9	14
10	Self-templated pseudomorphic transformation of ZIF into layered double hydroxides for improved supercapacitive performance. Journal of Colloid and Interface Science, 2022, 622, 309-318.	5.0	14
11	Metal-Organic Frameworks-derived Indium Clusters/Carbon Nanocomposites for Efficient CO2 Electroreduction. Chemical Research in Chinese Universities, 2022, 38, 1287-1291.	1.3	5
12	Dye-Encapsulated Lanthanide-Based Metal–Organic Frameworks as a Dual-Emission Sensitization Platform for Alachlor Sensing. Inorganic Chemistry, 2022, 61, 9801-9807.	1.9	9
13	Photothermalâ€Driven Highâ€Performance Selective Hydrogenation System Enabled by Delicately Designed IrCo Nanocages. Small, 2022, 18, .	5.2	2
14	Prussian blue and its analogues for aqueous energy storage: From fundamentals to advanced devices. Energy Storage Materials, 2022, 50, 618-640.	9.5	34
15	Ultraâ€Small Noble Metal Ceriaâ€Based Catalytic Materials: From Synthesis to Application. European Journal of Inorganic Chemistry, 2021, 2021, 689-701.	1.0	6
16	Recent Advances in Graphitic Carbon Nitride Supported Singleâ€Atom Catalysts for Energy Conversion. ChemCatChem, 2021, 13, 1250-1270.	1.8	46
17	Cancer therapeutic strategies based on metal ions. Chemical Science, 2021, 12, 12234-12247.	3.7	33
18	A Polymerâ€Assisted Spinodal Decomposition Strategy toward Interconnected Porous Sodium Super Ionic Conductorâ€Structured Polyanionâ€Type Materials and Their Application as a Highâ€Power Sodiumâ€Ion Battery Cathode. Advanced Science, 2021, 8, e2004943.	5.6	29

#	Article	IF	CITATIONS
19	Conjugated Microporous Polymers with Bipolar and Double Redoxâ€Active Centers for Highâ€Performance Dualâ€Ion, Organic Symmetric Battery. Advanced Energy Materials, 2021, 11, 2100381.	10.2	41
20	Layerâ€byâ€Layer Electrodeposition of FTO/TiO 2 /Cu x O/CeO 2 (1 < x < 2) Photocatalysts with High Peroxidaseâ€Like Activity by Greatly Enhanced Singlet Oxygen Generation. Small Methods, 2021, 5, 2100423.	4.6	11
21	Highly Active PdO/Mn ₃ O ₄ /CeO ₂ Nanocomposites Supported on One Dimensional Halloysite Nanotubes for Photoassisted Thermal Catalytic Methane Combustion. Angewandte Chemie - International Edition, 2021, 60, 18552-18556.	7.2	46
22	Highly Active PdO/Mn 3 O 4 /CeO 2 Nanocomposites Supported on One Dimensional Halloysite Nanotubes for Photoassisted Thermal Catalytic Methane Combustion. Angewandte Chemie, 2021, 133, 18700-18704.	1.6	2
23	Unraveling the physical chemistry and materials science of CeO2-based nanostructures. CheM, 2021, 7, 2022-2059.	5.8	64
24	Rational design of active layer configuration with parallel graphene/polyaniline composite films for high-performance supercapacitor electrode. Electrochimica Acta, 2021, 398, 139330.	2.6	17
25	Ballâ€Milling Induced Debonding of Surface Atoms from Metal Bulk for Construing Highâ€Performance Dualâ€Site Singleâ€Atom Catalysts. Angewandte Chemie, 2021, 133, 23338-23342.	1.6	27
26	Ballâ€Milling Induced Debonding of Surface Atoms from Metal Bulk for Construing Highâ€Performance Dualâ€ S ite Singleâ€Atom Catalysts. Angewandte Chemie - International Edition, 2021, 60, 23154-23158.	7.2	48
27	Salt-tolerant and low-cost flame-treated aerogel for continuously efficient solar steam generation. Solar Energy, 2021, 227, 303-311.	2.9	29
28	Insights into high CO-SCR performance of CuCoAlO catalysts derived from LDH/MOFs composites and study of H2O/SO2 and alkali metal resistance. Chemical Engineering Journal, 2021, 426, 131873.	6.6	50
29	Co ₃ O ₄ /CeO ₂ multi-shelled nanospheres derived from self-templated synthesis for efficient catalytic CO oxidation. Dalton Transactions, 2021, 50, 9637-9642.	1.6	6
30	Rapidly clearable MnCo ₂ O ₄ @PAA as novel nanotheranostic agents for T ₁ /T ₂ bimodal MRI imaging-guided photothermal therapy. Nanoscale, 2021, 13, 16251-16257.	2.8	8
31	Prussian Blue Analogs and Their Derived Nanomaterials for Electrochemical Energy Storage and Electrocatalysis. Small Methods, 2021, 5, e2001000.	4.6	81
32	Hierarchical MoO ₄ ^{2–} Intercalating α-Co(OH) ₂ Nanosheet Assemblies: Green Synthesis and Ultrafast Reconstruction for Boosting Electrochemical Oxygen Evolution. Energy & Fuels, 2021, 35, 2775-2784.	2.5	13
33	Optical fiber sensor based on upconversion nanoparticles for internal temperature monitoring of Li-ion batteries. Journal of Materials Chemistry C, 2021, 9, 14757-14765.	2.7	20
34	Tumor Diagnosis and Therapy Mediated by Metal Phosphorusâ€Based Nanomaterials. Advanced Materials, 2021, 33, e2103936.	11.1	31
35	Cobalt nanoparticle–carbon nanoplate as the solar absorber of a wood aerogel evaporator for continuously efficient desalination. Environmental Science: Water Research and Technology, 2021, 8, 151-161.	1.2	14
36	Robust Synthesis of Goldâ€Based Multishell Structures as Plasmonic Catalysts for Selective Hydrogenation of 4â€Nitrostyrene. Angewandte Chemie, 2020, 132, 1119-1123.	1.6	3

#	Article	IF	CITATIONS
37	Robust Synthesis of Goldâ€Based Multishell Structures as Plasmonic Catalysts for Selective Hydrogenation of 4â€Nitrostyrene. Angewandte Chemie - International Edition, 2020, 59, 1103-1107.	7.2	29
38	A redox interaction-engaged strategy for multicomponent nanomaterials. Chemical Society Reviews, 2020, 49, 736-764.	18.7	32
39	Specific Core–Satellite Nanocarriers for Enhanced Intracellular ROS Generation and Synergistic Photodynamic Therapy. ACS Applied Materials & Interfaces, 2020, 12, 5403-5412.	4.0	23
40	Catalytic activity boost of CeO ₂ /Co ₃ O ₄ nanospheres derived from CeCo-glycolate <i>via</i> yolk–shell structural evolution. Inorganic Chemistry Frontiers, 2020, 7, 421-426.	3.0	3
41	Smart Porous Core–Shell Cuprous Oxide Nanocatalyst with High Biocompatibility for Acidâ€Triggered Chemo/Chemodynamic Synergistic Therapy. Small, 2020, 16, e2001805.	5.2	109
42	Fabrication of a vanadium nitride/N-doped carbon hollow nanosphere composite as an efficient electrode material for asymmetric supercapacitors. Nanoscale Advances, 2020, 2, 3865-3871.	2.2	27
43	Multistimuli-Responsive Polymeric Vesicles for Accelerated Drug Release in Chemo-photothermal Therapy. ACS Biomaterials Science and Engineering, 2020, 6, 5012-5023.	2.6	20
44	Boosting Chemodynamic Therapy by the Synergistic Effect of Co-Catalyze and Photothermal Effect Triggered by the Second Near-Infrared Light. Nano-Micro Letters, 2020, 12, 180.	14.4	49
45	Na ₂ S ₂ O ₈ Nanoparticles Trigger Antitumor Immunotherapy through Reactive Oxygen Species Storm and Surge of Tumor Osmolarity. Journal of the American Chemical Society, 2020, 142, 21751-21757.	6.6	133
46	Dualâ€Defects Adjusted Crystalâ€Field Splitting of LaCo _{1â°'<i>x</i>} Ni _{<i>x</i>} O _{3â^'<i>δ</i>} Hollow Multishelled Structures for Efficient Oxygen Evolution. Angewandte Chemie - International Edition, 2020, 59, 19691-19695.	7.2	80
47	A Singleâ€Atom Manipulation Approach for Synthesis of Atomically Mixed Nanoalloys as Efficient Catalysts. Angewandte Chemie - International Edition, 2020, 59, 13568-13574.	7.2	23
48	A Singleâ€Atom Manipulation Approach for Synthesis of Atomically Mixed Nanoalloys as Efficient Catalysts. Angewandte Chemie, 2020, 132, 13670-13676.	1.6	8
49	In Situ Construction of Pt–Ni NF@Niâ€MOFâ€74 for Selective Hydrogenation of <i>p</i> â€Nitrostyrene by Ammonia Borane. Chemistry - A European Journal, 2020, 26, 12539-12543.	1.7	9
50	Ligand-Assisted Coordinative Self-Assembly Method to Synthesize Mesoporous Zn _{<i>x</i>} Cd _{1–<i>x</i>} S Nanospheres with Nano-Twin-Induced Phase Junction for Enhanced Photocatalytic H ₂ Evolution. Inorganic Chemistry, 2020, 59, 5063-5071.	1.9	19
51	A new perspective of lanthanide metal–organic frameworks: tailoring Dy-BTC nanospheres for rechargeable Li–O ₂ batteries. Nanoscale, 2020, 12, 9524-9532.	2.8	29
52	Dualâ€Defects Adjusted Crystalâ€Field Splitting of LaCo _{1â"<i>x</i>} Ni _{<i>x</i>} O _{3â"<i>î</i>} Hollow Multishelled Structures for Efficient Oxygen Evolution. Angewandte Chemie, 2020, 132, 19859-19863.	1.6	5
53	Bismuthene for highly efficient carbon dioxide electroreduction reaction. Nature Communications, 2020, 11, 1088.	5.8	278
54	In Situ Formation of Co ₉ S ₈ Quantum Dots in MOFâ€Đerived Ternary Metal Layered Double Hydroxide Nanoarrays for Highâ€Performance Hybrid Supercapacitors. Advanced Energy Materials, 2020, 10, 1903193.	10.2	138

#	Article	IF	CITATIONS
55	One-step co-precipitation synthesis of novel BiOCl/CeO ₂ composites with enhanced photodegradation of rhodamine B. Inorganic Chemistry Frontiers, 2020, 7, 1345-1361.	3.0	42
56	Defect modified zinc oxide with augmenting sonodynamic reactive oxygen species generation. Biomaterials, 2020, 251, 120075.	5.7	125
57	[(UO 2)(C 10 H 8 N 2 O 2) 2][HPW 12 O 40]: The First Case of a Uranyl Coordination Network Containing a Kegginâ€Type Polyoxometalate. European Journal of Inorganic Chemistry, 2020, 2020, 4577-4580.	1.0	3
58	Industrial carbon dioxide capture and utilization: state of the art and future challenges. Chemical Society Reviews, 2020, 49, 8584-8686.	18.7	610
59	Constructing radially oriented macroporous spheres with central cavities as ultrastable lithium-ion battery anodes. Energy Storage Materials, 2019, 17, 242-252.	9.5	23
60	Preparation and enhanced photocatalytic performance of sulfur doped terminal-methylated g-C ₃ N ₄ nanosheets with extended visible-light response. Journal of Materials Chemistry A, 2019, 7, 20640-20648.	5.2	105
61	Controllable Synthesis of Mesoporous TiO ₂ Polymorphs with Tunable Crystal Structure for Enhanced Photocatalytic H ₂ Production. Advanced Energy Materials, 2019, 9, 1901634.	10.2	131
62	Design strategies and applications of charged metal organic frameworks. Coordination Chemistry Reviews, 2019, 398, 113007.	9.5	72
63	Double Switch Biodegradable Porous Hollow Trinickel Monophosphide Nanospheres for Multimodal Imaging Guided Photothermal Therapy. Nano Letters, 2019, 19, 5093-5101.	4.5	64
64	Copper(I) Phosphide Nanocrystals for In Situ Selfâ€Generation Magnetic Resonance Imagingâ€Guided Photothermalâ€Enhanced Chemodynamic Synergetic Therapy Resisting Deepâ€Seated Tumor. Advanced Functional Materials, 2019, 29, 1904678.	7.8	185
65	Plasmonic Pt Superstructures with Boosted Nearâ€Infrared Absorption and Photothermal Conversion Efficiency in the Second Biowindow for Cancer Therapy. Advanced Materials, 2019, 31, e1904836.	11.1	105
66	CeO ₂ â€Encapsulated Hollow Ag–Au Nanocage Hybrid Nanostructures as Highâ€Performance Catalysts for Cascade Reactions. Small, 2019, 15, e1903182.	5.2	33
67	Photothermal-Enhanced Inactivation of Glutathione Peroxidase for Ferroptosis Sensitized by an Autophagy Promotor. ACS Applied Materials & Interfaces, 2019, 11, 42988-42997.	4.0	75
68	CO Oxidation Catalyzed by Two-Dimensional Co ₃ O ₄ /CeO ₂ Nanosheets. ACS Applied Nano Materials, 2019, 2, 5769-5778.	2.4	45
69	Clean synthesis of ZnCo2O4@ZnCo-LDHs yolk–shell nanospheres composed of ultra-thin nanosheets with enhanced electrocatalytic properties. Inorganic Chemistry Frontiers, 2019, 6, 220-225.	3.0	17
70	A Polymerâ€Oriented Selfâ€Assembly Strategy toward Mesoporous Metal Oxides with Ultrahigh Surface Areas. Advanced Science, 2019, 6, 1801543.	5.6	25
71	A ratiometric fluorescent sensor with dual response of Fe3+/Cu2+ based on europium post-modified sulfone-metal-organic frameworks and its logical application. Talanta, 2019, 197, 291-298.	2.9	57
72	A Bipolar and Selfâ€Polymerized Phthalocyanine Complex for Fast and Tunable Energy Storage in Dualâ€Ion Batteries. Angewandte Chemie - International Edition, 2019, 58, 10204-10208.	7.2	78

#	Article	IF	CITATIONS
73	A Bipolar and Selfâ€Polymerized Phthalocyanine Complex for Fast and Tunable Energy Storage in Dualâ€Ion Batteries. Angewandte Chemie, 2019, 131, 10310-10314.	1.6	24
74	Tunable bimetallic Au–Pd@CeO ₂ for semihydrogenation of phenylacetylene by ammonia borane. Nanoscale, 2019, 11, 12932-12937.	2.8	32
75	Metal–organic framework-based materials for the recovery of uranium from aqueous solutions. Inorganic Chemistry Frontiers, 2019, 6, 1924-1937.	3.0	108
76	Bimetallic NiCo2S4 Nanoneedles Anchored on Mesocarbon Microbeads as Advanced Electrodes for Asymmetric Supercapacitors. Nano-Micro Letters, 2019, 11, 35.	14.4	83
77	Syntheses and Applications of Noble-Metal-free CeO2-Based Mixed-Oxide Nanocatalysts. CheM, 2019, 5, 1743-1774.	5.8	125
78	Construction of trace silver modified core@shell structured Pt-Ni nanoframe@CeO2 for semihydrogenation of phenylacetylene. Nano Research, 2019, 12, 869-875.	5.8	27
79	Stimuli-responsive nanotheranostics based on lanthanide-doped upconversion nanoparticles for cancer imaging and therapy: current advances and future challenges. Nano Today, 2019, 25, 38-67.	6.2	100
80	Highâ€Performance Ultrathin Co ₃ O ₄ Nanosheet Supported PdO/CeO ₂ Catalysts for Methane Combustion. Advanced Energy Materials, 2019, 9, 1803583.	10.2	57
81	Catalytic Mechanisms of Nanozymes and Their Applications in Biomedicine. Bioconjugate Chemistry, 2019, 30, 1273-1296.	1.8	113
82	Half-Encapsulated Au Nanorods@CeO ₂ Core@Shell Nanostructures for Near-Infrared Plasmon-Enhanced Catalysis. ACS Applied Nano Materials, 2019, 2, 1516-1524.	2.4	34
83	CeO ₂ supported low-loading Au as an enhanced catalyst for low temperature oxidation of carbon monoxide. CrystEngComm, 2019, 21, 7108-7113.	1.3	12
84	Oneâ€Dimensional Fe ₂ P Acts as a Fenton Agent in Response to NIRâ€II Light and Ultrasound for Deep Tumor Synergetic Theranostics. Angewandte Chemie, 2019, 131, 2429-2434.	1.6	44
85	Oneâ€Dimensional Fe ₂ P Acts as a Fenton Agent in Response to NIRâ€II Light and Ultrasound for Deep Tumor Synergetic Theranostics. Angewandte Chemie - International Edition, 2019, 58, 2407-2412.	7.2	315
86	Molecular Engineering of Monodisperse SnO ₂ Nanocrystals Anchored on Doped Graphene with Highâ€Performance Lithium/Sodium‧torage Properties in Half/Full Cells. Advanced Energy Materials, 2019, 9, 1802993.	10.2	129
87	Prevention of dendrite growth and volume expansion to give high-performance aprotic bimetallic Li-Na alloy–O2 batteries. Nature Chemistry, 2019, 11, 64-70.	6.6	265
88	Synthesis of hierarchically double-walled Co3O4 hollow nanofibers assembled by nanosheet building units supporting Pt nanoparticles for high-efficient CO oxidation. Materials Letters, 2019, 237, 126-129.	1.3	7
89	Hollow Multishelled Structure of Heterogeneous Co ₃ O ₄ –CeO _{2â^'} <i>_x</i> Nanocomposite for CO Catalytic Oxidation. Advanced Functional Materials, 2019, 29, 1806588.	7.8	86
90	Four new water-stable metal-organic frameworks based on diverse metal clusters: Syntheses, structures, and luminescent sensing properties. Journal of Solid State Chemistry, 2019, 269, 386-395.	1.4	10

#	Article	IF	CITATIONS
91	DFT and TDâ€DFT study of iridium complexes with lowâ€colorâ€temperature and lowâ€efficiency rollâ€off properties. Applied Organometallic Chemistry, 2019, 33, e4563.	1.7	5
92	Alkali Metal Anodes for Rechargeable Batteries. CheM, 2019, 5, 313-338.	5.8	170
93	Thermally Responsive Materials for Bioimaging. Chemistry - an Asian Journal, 2019, 14, 67-75.	1.7	11
94	A chelation-induced cooperative self-assembly methodology for the synthesis of mesoporous metal hydroxide and oxide nanospheres. Nanoscale, 2018, 10, 5731-5737.	2.8	21
95	Nanoporous Carbon-Coated Bimetallic Phosphides for Efficient Electrochemical Water Splitting. Crystal Growth and Design, 2018, 18, 3404-3410.	1.4	19
96	Co ₉ S ₈ Nanoparticlesâ€Embedded N/Sâ€Codoped Carbon Nanofibers Derived from Metal–Organic Frameworkâ€Wrapped CdS Nanowires for Efficient Oxygen Evolution Reaction. Small, 2018, 14, e1704035.	5.2	115
97	Ultrathin Porous NiFeV Ternary Layer Hydroxide Nanosheets as a Highly Efficient Bifunctional Electrocatalyst for Overall Water Splitting. Small, 2018, 14, 1703257.	5.2	279
98	Investigating the Hybridâ€Structureâ€Effect of CeO ₂ â€Encapsulated Au Nanostructures on the Transfer Coupling of Nitrobenzene. Advanced Materials, 2018, 30, 1704416.	11.1	57
99	Bloodâ€Capillaryâ€Inspired, Freeâ€Standing, Flexible, and Lowâ€Cost Superâ€Hydrophobic Nâ€CNTs@SS Cathc for Highâ€Capacity, Highâ€Rate, and Stable Liâ€Air Batteries. Advanced Energy Materials, 2018, 8, 1702242.	des 10.2	108
100	A New Coâ€P Nanocomposite with Ultrahigh Relaxivity for In Vivo Magnetic Resonance Imagingâ€Guided Tumor Eradication by Chemo/Photothermal Synergistic Therapy. Small, 2018, 14, 1702431.	5.2	29
101	All-in-One Theranostic Nanoagent with Enhanced Reactive Oxygen Species Generation and Modulating Tumor Microenvironment Ability for Effective Tumor Eradication. ACS Nano, 2018, 12, 4886-4893.	7.3	510
102	In Situ Generation of Bifunctional, Efficient Fe-Based Catalysts from Mackinawite Iron Sulfide for Water Splitting. CheM, 2018, 4, 1139-1152.	5.8	271
103	Multifunctional Cu–Ag ₂ S nanoparticles with high photothermal conversion efficiency for photoacoustic imaging-guided photothermal therapy <i>in vivo</i> . Nanoscale, 2018, 10, 825-831.	2.8	68
104	Tin Diselenide Molecular Precursor for Solutionâ€Processable Thermoelectric Materials. Angewandte Chemie, 2018, 130, 17309-17314.	1.6	9
105	Tin Diselenide Molecular Precursor for Solutionâ€Processable Thermoelectric Materials. Angewandte Chemie - International Edition, 2018, 57, 17063-17068.	7.2	23
106	Thermal Decomposition of CdS Nanowires Assisted by ZIF-67 to Induce the Formation of Co ₉ S ₈ -Based Carbon Nanomaterials with High Lithium-Storage Abilities. ACS Applied Energy Materials, 2018, 1, 6242-6249.	2.5	8
107	A bimetallic oxide Fe1.89Mo4.11O7 electrocatalyst with highly efficient hydrogen evolution reaction activity in alkaline and acidic media. Chemical Science, 2018, 9, 5640-5645.	3.7	38
108	Metal–Organic Framework Hybridâ€Assisted Formation of Co ₃ O ₄ /Coâ€Fe Oxide Doubleâ€6helled Nanoboxes for Enhanced Oxygen Evolution. Advanced Materials, 2018, 30, e1801211.	11.1	374

#	Article	IF	CITATIONS
109	Metal organic framework derived CoFe@N-doped carbon/reduced graphene sheets for enhanced oxygen evolution reaction. Inorganic Chemistry Frontiers, 2018, 5, 1962-1966.	3.0	34
110	Surface Sulfurization of NiCo-Layered Double Hydroxide Nanosheets Enable Superior and Durable Oxygen Evolution Electrocatalysis. ACS Applied Energy Materials, 2018, 1, 4040-4049.	2.5	71
111	Pt/CeO ₂ @MOF Core@Shell Nanoreactor for Selective Hydrogenation of Furfural via the Channel Screening Effect. ACS Catalysis, 2018, 8, 8506-8512.	5.5	145
112	A general one-pot strategy for the synthesis of Au@multi-oxide yolk@shell nanospheres with enhanced catalytic performance. Chemical Science, 2018, 9, 7569-7574.	3.7	35
113	Surfactantâ€Guided Synthesis of Porous Pt Shells with Ordered Tangential Channels, Coated on Pd Nanostructures, and Their Enhanced Catalytic Activities. Chemistry - A European Journal, 2018, 24, 15649-15655.	1.7	7
114	Coral-like cobaltous sulfide/N,S-codoped carbon with hierarchical pores as highly efficient noble metal-free electrocatalyst for oxygen reduction reactions. Journal of Alloys and Compounds, 2018, 769, 801-807.	2.8	10
115	Reduced graphene oxide nanosheet modified NiMn-LDH nanoflake arrays for high-performance supercapacitors. Chemical Communications, 2018, 54, 10172-10175.	2.2	46
116	Remote manipulation of upconversion luminescence. Chemical Society Reviews, 2018, 47, 6473-6485.	18.7	210
117	Hierarchical Bi ₂ Te ₃ Nanostrings: Green Synthesis and Their Thermoelectric Properties. Chemistry - A European Journal, 2018, 24, 9765-9768.	1.7	9
118	A Controllable Surface Etching Strategy for Wellâ€Đefined Spiny Yolk@Shell CuO@CeO ₂ Cubes and Their Catalytic Performance Boost. Advanced Functional Materials, 2018, 28, 1802559.	7.8	60
119	Corrosion engineering towards efficient oxygen evolution electrodes with stable catalytic activity for over 6000 hours. Nature Communications, 2018, 9, 2609.	5.8	389
120	Coupling Subâ€Nanometric Copper Clusters with Quasiâ€Amorphous Cobalt Sulfide Yields Efficient and Robust Electrocatalysts for Water Splitting Reaction. Advanced Materials, 2017, 29, 1606200.	11.1	350
121	Self-supported Co3O4wire-penetrated-cage hybrid arrays with enhanced supercapacitance properties. CrystEngComm, 2017, 19, 1459-1463.	1.3	11
122	Multishelled Ni <i> _x </i> Co ₃₋ <i> _x </i> O ₄ Hollow Microspheres Derived from Bimetal-Organic Frameworks as Anode Materials for High-Performance Lithium-Ion Batteries. Small, 2017, 13, 1604270.	5.2	120
123	Syntheses, structures, and magnetic properties of cobalt(II) and nickel(II) coordination polymers based on a V-shaped ligand. Journal of Solid State Chemistry, 2017, 250, 6-13.	1.4	3
124	Highly efficient heterogeneous catalytic materials derived from metal-organic framework supports/precursors. Coordination Chemistry Reviews, 2017, 337, 80-96.	9.5	282
125	Highâ€Performance Integrated Selfâ€Package Flexible Li–O ₂ Battery Based on Stable Composite Anode and Flexible Gas Diffusion Layer. Advanced Materials, 2017, 29, 1700378.	11.1	72
126	Bottom-up engineering of thermoelectric nanomaterials and devices from solution-processed nanoparticle building blocks. Chemical Society Reviews, 2017, 46, 3510-3528.	18.7	184

#	Article	IF	CITATIONS
127	Proton-conducting crystalline porous materials. Chemical Society Reviews, 2017, 46, 464-480.	18.7	530
128	A Simple Strategy for the Controlled Synthesis of Ultrasmall Hexagonalâ€Phase NaYF ₄ :Yb,Er Upconversion Nanocrystals. ChemPhotoChem, 2017, 1, 369-375.	1.5	18
129	PEGylated GdF ₃ :Fe Nanoparticles as Multimodal <i>T</i> ₁ / <i>T</i> ₂ -Weighted MRI and X-ray CT Imaging Contrast Agents. ACS Applied Materials & Interfaces, 2017, 9, 20426-20434.	4.0	45
130	Multifunctional core/satellite polydopamine@Nd3+-sensitized upconversion nanocomposite: A single 808 nm near-infrared light-triggered theranostic platform for in vivo imaging-guided photothermal therapy. Nano Research, 2017, 10, 3434-3446.	5.8	69
131	Selfâ€Assembled Pd@CeO ₂ /γâ€Al ₂ O ₃ Catalysts with Enhanced Activity for Catalytic Methane Combustion. Small, 2017, 13, 1700941.	5.2	40
132	S,N co-doped carbon nanotubes decorated with ultrathin molybdenum disulfide nanosheets with highly electrochemical performance. Nanoscale, 2017, 9, 6346-6352.	2.8	20
133	Ultrafast Formation of Amorphous Bimetallic Hydroxide Films on 3D Conductive Sulfide Nanoarrays for Large urrentâ€Đensity Oxygen Evolution Electrocatalysis. Advanced Materials, 2017, 29, 1700404.	11.1	462
134	Catalytically active Co 3 O 4 hybrid microstructures and their morphology evolution induced by ceria. Materials Research Bulletin, 2017, 96, 2-9.	2.7	5
135	Achieving the Tradeâ€Off between Selectivity and Activity in Semihydrogenation of Alkynes by Fabrication of (Asymmetrical Pd@Ag Core)@(CeO ₂ Shell) Nanocatalysts via Autoredox Reaction. Advanced Materials, 2017, 29, 1605332.	11.1	73
136	Binary temporal upconversion codes of Mn2+-activated nanoparticles for multilevel anti-counterfeiting. Nature Communications, 2017, 8, 899.	5.8	290
137	Flexible Electrodes for Sodiumâ€lon Batteries: Recent Progress and Perspectives. Advanced Materials, 2017, 29, 1703012.	11.1	156
138	Ultrafast Synthesis of Ultrasmall Poly(Vinylpyrrolidone)â€Protected Bismuth Nanodots as a Multifunctional Theranostic Agent for In Vivo Dualâ€Modal CT/Photothermalâ€Imagingâ€Guided Photothermal Therapy. Advanced Functional Materials, 2017, 27, 1702018.	7.8	203
139	Formation of Septupleâ€Shelled (Co _{2/3} Mn _{1/3})(Co _{5/6} Mn _{1/6}) ₂ O ₄ Hollow Spheres as Electrode Material for Alkaline Rechargeable Battery. Advanced Materials, 2017, 29, 1700550.	11.1	122
140	Preparation of Carbonâ€Rich <i>g</i> ₃ N ₄ Nanosheets with Enhanced Visible Light Utilization for Efficient Photocatalytic Hydrogen Production. Small, 2017, 13, 1701552.	5.2	142
141	Confining the Nucleation of Pt to In Situ Form (Ptâ€Enriched Cage)@CeO ₂ Core@Shell Nanostructure as Excellent Catalysts for Hydrogenation Reactions. Advanced Materials, 2017, 29, 1700495.	11.1	72
142	Solid ion transition route to 3D S–N-codoped hollow carbon nanosphere/graphene aerogel as a metal-free handheld nanocatalyst for organic reactions. Nano Research, 2017, 10, 3486-3495.	5.8	14
143	Oneâ€Pot Synthesis of Cobaltâ€Doped Pt–Au Alloy Nanoparticles Supported on Ultrathin αâ€Co(OH) ₂ Nanosheets and Their Enhanced Performance in the Reduction of <i>p</i> â€Nitrophenol. European Journal of Inorganic Chemistry, 2017, 2017, 146-152.	1.0	8
144	Electrochemical Reduction of N ₂ under Ambient Conditions for Artificial N ₂ Fixation and Renewable Energy Storage Using N ₂ /NH ₃ Cycle. Advanced Materials, 2017, 29, 1604799.	11.1	969

#	Article	IF	CITATIONS
145	Surfactantâ€Free Aqueous Synthesis of Pure Singleâ€Crystalline SnSe Nanosheet Clusters as Anode for High Energy―and Powerâ€Density Sodiumâ€Ion Batteries. Advanced Materials, 2017, 29, 1602469.	11.1	231
146	Formation of Onionâ€Like NiCo ₂ S ₄ Particles via Sequential Ionâ€Exchange for Hybrid Supercapacitors. Advanced Materials, 2017, 29, 1605051.	11.1	539
147	Green self-redox synthesis of Rh-PPy-RGO ternary nanocomposite with highly increased catalytic performances. Main Group Chemistry, 2017, 16, 199-206.	0.4	1
148	<scp>l</scp> â€Arginineâ€Triggered Selfâ€Assembly of CeO ₂ Nanosheaths on Palladium Nanoparticles in Water. Angewandte Chemie, 2016, 128, 4618-4622.	1.6	11
149	Polydopamine coated manganese oxide nanoparticles with ultrahigh relaxivity as nanotheranostic agents for magnetic resonance imaging guided synergetic chemo-/photothermal therapy. Chemical Science, 2016, 7, 6695-6700.	3.7	116
150	Acid–Baseâ€Triggered Structural Transformation of a Polyoxometalate Core Inside a Dodecahedraneâ€ŀike Silver Thiolate Shell. Angewandte Chemie - International Edition, 2016, 55, 3699-3703.	7.2	106
151	A Metal–Organic Framework/DNA Hybrid System as a Novel Fluorescent Biosensor for Mercury(II) Ion Detection. Chemistry - A European Journal, 2016, 22, 477-480.	1.7	155
152	Innenrücktitelbild:l-Arginine-Triggered Self-Assembly of CeO2Nanosheaths on Palladium Nanoparticles in Water (Angew. Chem. 14/2016). Angewandte Chemie, 2016, 128, 4687-4687.	1.6	0
153	In situ loading of Ag2WO4 on ultrathin g-C3N4 nanosheets with highly enhanced photocatalytic performance. Journal of Hazardous Materials, 2016, 313, 219-228.	6.5	135
154	A Family of Metal–Organic Frameworks with a New Chair-Conformation Resorcin[4]arene-Based Ligand: Selective Luminescent Sensing of Amine and Aldehyde Vapors, and Solvent-Mediated Structural Transformations. Crystal Growth and Design, 2016, 16, 3244-3255.	1.4	45
155	Rational design of Nd ³⁺ -sensitized multifunctional nanoparticles with highly dominant red emission. Dalton Transactions, 2016, 45, 8440-8446.	1.6	8
156	Optimization of Bi ³⁺ in Upconversion Nanoparticles Induced Simultaneous Enhancement of Near-Infrared Optical and X-ray Computed Tomography Imaging Capability. ACS Applied Materials & Interfaces, 2016, 8, 27490-27497.	4.0	72
157	A Porphyrinâ€Based Porous <i>rtl</i> Metal–Organic Framework as an Efficient Catalyst for the Cycloaddition of CO ₂ to Epoxides. Chemistry - A European Journal, 2016, 22, 16991-16997.	1.7	61
158	A Flexible and Wearable Lithium–Oxygen Battery with Record Energy Density achieved by the Interlaced Architecture inspired by Bamboo Slips. Advanced Materials, 2016, 28, 8413-8418.	11.1	138
159	Macroscopic Foam‣ike Holey Ultrathin gâ€C ₃ N ₄ Nanosheets for Drastic Improvement of Visible‣ight Photocatalytic Activity. Advanced Energy Materials, 2016, 6, 1601273.	10.2	466
160	Cathode Surfaceâ€Induced, Solvationâ€Mediated, Micrometerâ€5ized Li ₂ O ₂ Cycling for Li–O ₂ Batteries. Advanced Materials, 2016, 28, 9620-9628.	11.1	232
161	A "Solid Dualâ€lonsâ€Transformation―Route to S,N Coâ€Doped Carbon Nanotubes as Highly Efficient "Metalâ€Free―Catalysts for Organic Reactions. Advanced Materials, 2016, 28, 10679-10683.	11.1	107
162	Multi-shelled metal oxides prepared via an anion-adsorption mechanism for lithium-ion batteries. Nature Energy, 2016, 1, .	19.8	352

#	Article	IF	CITATIONS
163	Designed synthesis of multi-functional PEGylated Yb ₂ O ₃ :Gd@SiO ₂ @CeO ₂ islands core@shell nanostructure. Dalton Transactions, 2016, 45, 11522-11527.	1.6	5
164	Core–shell–shell heterostructures of α-NaLuF ₄ :Yb/Er@NaLuF ₄ :Yb@MF ₂ (M = Ca, Sr, Ba) with remarkably enhanced upconversion luminescence. Dalton Transactions, 2016, 45, 11129-11136.	1.6	15
165	In situ redox strategy for large-scale fabrication of surfactant-free M-Fe2O3 (M = Pt, Pd, Au) hybrid nanospheres. Science China Materials, 2016, 59, 191-199.	3.5	9
166	Acid–Baseâ€Triggered Structural Transformation of a Polyoxometalate Core Inside a Dodecahedraneâ€like Silver Thiolate Shell. Angewandte Chemie, 2016, 128, 3763-3767.	1.6	35
167	<scp>l</scp> â€Arginineâ€Triggered Selfâ€Assembly of CeO ₂ Nanosheaths on Palladium Nanoparticles in Water. Angewandte Chemie - International Edition, 2016, 55, 4542-4546.	7.2	63
168	Reduced Grapheneâ€Wrapped MnO ₂ Nanowires Selfâ€Inserted with Co ₃ O ₄ Nanocages: Remarkable Enhanced Performances for Lithiumâ€Ion Anode Applications. Chemistry - A European Journal, 2016, 22, 6876-6880.	1.7	18
169	Dual-functional α-NaYb(Mn)F4:Er3+@NaLuF4 nanocrystals with highly enhanced red upconversion luminescence. RSC Advances, 2016, 6, 33493-33500.	1.7	5
170	Nanoconfined nitrogen-doped carbon-coated MnO nanoparticles in graphene enabling high performance for lithium-ion batteries and oxygen reduction reaction. Chemical Science, 2016, 7, 4284-4290.	3.7	121
171	An ideal detector composed of a 3D Gd-based coordination polymer for DNA and Hg ²⁺ ion. Inorganic Chemistry Frontiers, 2016, 3, 376-380.	3.0	37
172	Lanthanide doped Bi ₂ O ₃ upconversion luminescence nanospheres for temperature sensing and optical imaging. Dalton Transactions, 2016, 45, 2686-2693.	1.6	67
173	Decoration of Pt on Cu/Co double-doped CeO ₂ nanospheres and their greatly enhanced catalytic activity. Chemical Science, 2016, 7, 1867-1873.	3.7	51
174	CeO ₂ nanowires self-inserted into porous Co ₃ O ₄ frameworks as high-performance "noble metal free―hetero-catalysts. Chemical Science, 2016, 7, 1109-1114.	3.7	74
175	Frequency Specificity of fMRI in Mesial Temporal Lobe Epilepsy. PLoS ONE, 2016, 11, e0157342.	1.1	9
176	ZnOâ€Functionalized Upconverting Nanotheranostic Agent: Multiâ€Modality Imagingâ€Guided Chemotherapy with Onâ€Demand Drug Release Triggered by pH. Angewandte Chemie - International Edition, 2015, 54, 536-540.	7.2	131
177	Energy Migration Upconversion in Manganese(II)â€Doped Nanoparticles. Angewandte Chemie - International Edition, 2015, 54, 13312-13317.	7.2	64
178	Encapsulation of Ln ^{III} Ions/Dyes within a Microporous Anionic MOF by Postâ€synthetic Ionic Exchange Serving as a Ln ^{III} Ion Probe and Two olor Luminescent Sensors. Chemistry - A European Journal, 2015, 21, 9748-9752.	1.7	123
179	Strongly Coupled Pt–Ni ₂ GeO ₄ Hybrid Nanostructures as Potential Nanocatalysts for CO Oxidation. Chemistry - A European Journal, 2015, 21, 14768-14771.	1.7	5
180	Ultrathin g < ₃ N ₄ Nanosheets Coupled with AgIO ₃ as Highly Efficient Heterostructured Photocatalysts for Enhanced Visible‣ight Photocatalytic Activity. Chemistry - A European Journal, 2015, 21, 17739-17747.	1.7	40

#	Article	IF	CITATIONS
181	Sandwich‧tructured Graphene–Nickel Silicate–Nickel Ternary Composites as Superior Anode Materials for Lithiumâ€lon Batteries. Chemistry - A European Journal, 2015, 21, 9014-9017.	1.7	32
182	Structural design of graphene for use in electrochemical energy storage devices. Chemical Society Reviews, 2015, 44, 6230-6257.	18.7	389
183	Yb ³⁺ /Er ³⁺ -Codoped Bi ₂ O ₃ Nanospheres: Probe for Upconversion Luminescence Imaging and Binary Contrast Agent for Computed Tomography Imaging. ACS Applied Materials & Interfaces, 2015, 7, 26346-26354.	4.0	78
184	Two-dimensional NiCo ₂ O ₄ nanosheet-coated three-dimensional graphene networks for high-rate, long-cycle-life supercapacitors. Nanoscale, 2015, 7, 7035-7039.	2.8	134
185	Facile Synthesis of Hierarchical Magnesium Silicate Hollow Nanofibers Assembled by Nanosheets as an Efficient Adsorbent. ChemPlusChem, 2015, 80, 544-548.	1.3	19
186	Faceted Cu ₂ O structures with enhanced Li-ion battery anode performances. CrystEngComm, 2015, 17, 2110-2117.	1.3	69
187	Highly thermostable lanthanide metal–organic frameworks exhibiting unique selectivity for nitro explosives. RSC Advances, 2015, 5, 93-98.	1.7	46
188	Lanthanide Ion Codoped Emitters for Tailoring Emission Trajectory and Temperature Sensing. Advanced Functional Materials, 2015, 25, 1463-1469.	7.8	263
189	Rhâ€Niâ€B Nanoparticles as Highly Efficient Catalysts for Hydrogen Generation from Hydrous Hydrazine. Advanced Energy Materials, 2015, 5, 1401879.	10.2	61
190	A Family of Capsule-Based Coordination Polymers Constructed from a New Tetrakis(1,2,4-triazol-ylmethyl)resorcin[4]arene Cavitand and Varied Dicarboxylates for Selective Metal-Ion Exchange and Luminescent Properties. Crystal Growth and Design, 2015, 15, 3822-3831.	1.4	43
191	Growth of lanthanide-doped LiGdF4 nanoparticles induced by LiLuF4 core as tri-modal imaging bioprobes. Biomaterials, 2015, 65, 115-123.	5.7	55
192	Two new tetrazamacrocycle based Cu(II) complexes with 2D→0D single-crystal to single-crystal transformation. Inorganic Chemistry Communication, 2015, 57, 26-28.	1.8	2
193	Copper Salts Mediated Morphological Transformation of Cu2O from Cubes to Hierarchical Flower-like or Microspheres and Their Supercapacitors Performances. Scientific Reports, 2015, 5, 9672.	1.6	90
194	Microwave-assisted synthesis of nanoscale Eu(BTC)(H2O)·DMF with tunable luminescence. Science China Chemistry, 2015, 58, 973-978.	4.2	13
195	Noble metal-free hydrogen evolution catalysts for water splitting. Chemical Society Reviews, 2015, 44, 5148-5180.	18.7	4,776
196	CeO2-encapsulated noble metal nanocatalysts: enhanced activity and stability for catalytic application. NPG Asia Materials, 2015, 7, e179-e179.	3.8	101
197	A tetranuclear copper cluster-based MOF with sulfonate–carboxylate ligands exhibiting high proton conduction properties. Chemical Communications, 2015, 51, 8150-8152.	2.2	96
198	A Temperatureâ€Responsive Smart Europium Metalâ€Organic Framework Switch for Reversible Capture and Release of Intrinsic Eu ³⁺ Ions. Advanced Science, 2015, 2, 1500012.	5.6	83

#	Article	IF	CITATIONS
199	Fe3O4-nanoparticle-decorated TiO2 nanofiber hierarchical heterostructures with improved lithium-ion battery performance over wide temperature range. Nano Research, 2015, 8, 1659-1668.	5.8	33
200	Copper doped ceria porous nanostructures towards a highly efficient bifunctional catalyst for carbon monoxide and nitric oxide elimination. Chemical Science, 2015, 6, 2495-2500.	3.7	74
201	Pt nanohelices with highly ordered horizontal pore channels as enhanced photothermal materials. Chemical Science, 2015, 6, 6420-6424.	3.7	23
202	α-NaYb(Mn)F ₄ :Er ³⁺ /Tm ³⁺ @NaYF ₄ UCNPs as "Band-Shape―Luminescent Nanothermometers over a Wide Temperature Range. ACS Applied Materials & Interfaces, 2015, 7, 20813-20819.	4.0	114
203	Mesoporous TiO ₂ -Based Photoanode Sensitized by BiOI and Investigation of Its Photovoltaic Behavior. Langmuir, 2015, 31, 10279-10284.	1.6	57
204	Galvanic replacement synthesis of Ag _x Au _{1â^'x} @CeO ₂ (0 ≤ ≤) core@shell nanospheres with greatly enhanced catalytic performance. Chemical Science, 2015, 6, 7015-7019.	3.7	29
205	Cubic KLu ₃ F ₁₀ nanocrystals: Mn ²⁺ dopant-controlled synthesis and upconversion luminescence. Dalton Transactions, 2015, 44, 17286-17292.	1.6	12
206	Beyond graphene: materials chemistry toward high performance inorganic functional materials. Journal of Materials Chemistry A, 2015, 3, 2441-2453.	5.2	69
207	Preparation and enhanced visible light photocatalytic activity of novel g-C ₃ N ₄ nanosheets loaded with Ag ₂ CO ₃ nanoparticles. Nanoscale, 2015, 7, 758-764.	2.8	166
208	Assembly of three coordination polymers based on a sulfonic–carboxylic ligand showing high proton conductivity. Dalton Transactions, 2015, 44, 948-954.	1.6	53
209	Injection, transport, absorption and phosphorescence properties of a series of platinum (II) complexes with N-heterocyclic carbenes: a DFT and time-dependent DFT study. Journal of Molecular Modeling, 2014, 20, 2437.	0.8	2
210	Co ₃ O ₄ @CeO ₂ Core@Shell Cubes: Designed Synthesis and Optimization of Catalytic Properties. Chemistry - A European Journal, 2014, 20, 4469-4473.	1.7	75
211	A Eu/Tb-codoped coordination polymer luminescent thermometer. Inorganic Chemistry Frontiers, 2014, 1, 757-760.	3.0	63
212	A long-wave optical pH sensor based on red upconversion luminescence of NaGdF ₄ nanotubes. RSC Advances, 2014, 4, 55897-55899.	1.7	16
213	Singleâ€Crystalâ€ŧoâ€Singleâ€Crystal Transformation of a Europium(III) Metal–Organic Framework Producing a Multiâ€responsive Luminescent Sensor. Advanced Functional Materials, 2014, 24, 4034-4041.	7.8	542
214	A new type of double-chain based 3D lanthanide(iii) metal–organic framework demonstrating proton conduction and tunable emission. Chemical Communications, 2014, 50, 1912.	2.2	118
215	Constructing porous MOF based on the assembly of layer framework and p-sulfonatocalix[4]arene nanocapsule with proton-conductive property. CrystEngComm, 2014, 16, 64-68.	1.3	31
216	A europium(<scp>iii</scp>) based metal–organic framework: bifunctional properties related to sensing and electronic conductivity. Journal of Materials Chemistry A, 2014, 2, 237-244.	5.2	149

#	Article	IF	CITATIONS
217	Preciousâ€Metalâ€Free Nanocatalysts for Highly Efficient Hydrogen Production from Hydrous Hydrazine. Advanced Functional Materials, 2014, 24, 7073-7077.	7.8	14
218	Fe ₃ O ₄ @SiO ₂ @TiO ₂ @Pt Hierarchical Core–Shell Microspheres: Controlled Synthesis, Enhanced Degradation System, and Rapid Magnetic Separation to Recycle. Crystal Growth and Design, 2014, 14, 5506-5511.	1.4	77
219	Luminescent Lanthanide Metal–Organic Frameworks. Structure and Bonding, 2014, , 109-144.	1.0	20
220	Polymorphic crystallization of Cu ₂ O compound. CrystEngComm, 2014, 16, 5257-5267.	1.3	47
221	In situ generated FeF 3 in homogeneous iron matrix toward high-performance cathode material for sodium-ion batteries. Nano Energy, 2014, 10, 295-304.	8.2	101
222	Crystallization of Fe3+ in an alkaline aqueous pseudocapacitor system. CrystEngComm, 2014, 16, 6707.	1.3	27
223	Water crystallization to create ice spacers between graphene oxide sheets for highly electroactive graphene paper. CrystEngComm, 2014, 16, 7771.	1.3	47
224	A stable, pillar-layer metal–organic framework containing uncoordinated carboxyl groups for separation of transition metal ions. Chemical Communications, 2014, 50, 6406-6408.	2.2	76
225	Four coordination polymers constructed by a novel octacarboxylate functionalized calix[4]arene ligand: syntheses, structures, and photoluminescence property. CrystEngComm, 2014, 16, 9939-9946.	1.3	29
226	Multifunctional nanostructures based on porous silica covered Fe3O4@CeO2–Pt composites: a thermally stable and magnetically-recyclable catalyst system. Chemical Communications, 2014, 50, 7198.	2.2	29
227	In situ assembly of well-dispersed gold nanoparticles on hierarchical double-walled nickel silicate hollow nanofibers as an efficient and reusable hydrogenation catalyst. Chemical Communications, 2014, 50, 5447-5450.	2.2	31
228	Pure and intense orange upconversion luminescence of Eu3+ from the sensitization of Yb3+–Mn2+ dimer in NaY(Lu)F4 nanocrystals. Journal of Materials Chemistry C, 2014, 2, 9004-9011.	2.7	38
229	An unusual lamellar framework constructed from a tetracarboxylatocalix[4]arene with highly efficient metal-ion exchange. CrystEngComm, 2014, 16, 9520-9527.	1.3	12
230	Facile Synthesis and Properties of Hierarchical Double-Walled Copper Silicate Hollow Nanofibers Assembled by Nanotubes. ACS Nano, 2014, 8, 3664-3670.	7.3	80
231	An ionic aqueous pseudocapacitor system: electroactive ions in both a salt electrode and redox electrolyte. RSC Advances, 2014, 4, 23338.	1.7	57
232	Baclofen for stroke patients with persistent hiccups: a randomized, double-blind, placebo-controlled trial. Trials, 2014, 15, 295.	0.7	42
233	Fabrication of TiO ₂ –BiOCl double-layer nanostructure arrays for photoelectrochemical water splitting. CrystEngComm, 2014, 16, 820-825.	1.3	54
234	One-step synthesis of water-soluble hexagonal NaScF4:Yb/Er nanocrystals with intense red emission. Dalton Transactions, 2014, 43, 10202.	1.6	38

SHUYAN SONG

#	Article	IF	CITATIONS
235	Photophysical properties and theoretical calculations of Cu(I) dendrimers. Journal of Luminescence, 2014, 148, 103-110.	1.5	2
236	Metal-decorated Ni7S6 composite microflowers: Synthesis, characterization, and application. Materials Research Bulletin, 2014, 53, 199-204.	2.7	5
237	Luminescent Anionic Metal–Organic Framework with Potential Nitrobenzene Sensing. Crystal Growth and Design, 2014, 14, 3174-3178.	1.4	126
238	Rare earth fluorides upconversion nanophosphors: from synthesis to applications in bioimaging. CrystEngComm, 2013, 15, 7142.	1.3	54
239	Design and Synthesis of Enantiomerically Pure Chiral Sandwichlike Lamellar Structure: New Explorations from Molecular Building Blocks to Three-Dimensional Morphology. Crystal Growth and Design, 2013, 13, 976-980.	1.4	7
240	Graphene oxide covalently grafted upconversion nanoparticles for combined NIR mediated imaging and photothermal/photodynamic cancer therapy. Biomaterials, 2013, 34, 7715-7724.	5.7	344
241	Employing tripodal carboxylate ligand to construct Co(ii) coordination networks modulated by N-donor ligands: syntheses, structures and magnetic properties. Dalton Transactions, 2013, 42, 13231.	1.6	24
242	Single-crystalline CuGeO3 nanorods: Synthesis, characterization and properties. Materials Research Bulletin, 2013, 48, 2654-2660.	2.7	15
243	Synthesis of hexagonal Zn3(OH)2V2O7·2H2O nanoplates by a hydrothermal approach: Magnetic and photocatalytic properties. Materials Characterization, 2013, 86, 139-145.	1.9	14
244	Reversible Phase Transfer of Luminescent ZnO Quantum Dots between Polar and Nonpolar Media. Chemistry - A European Journal, 2013, 19, 6329-6333.	1.7	26
245	Chemical reaction controlled synthesis of Cu2O hollow octahedra and core–shell structures. CrystEngComm, 2013, 15, 10028.	1.3	45
246	Water-soluble inorganic salts with ultrahigh specific capacitance: crystallization transformation investigation of CuCl2 electrodes. CrystEngComm, 2013, 15, 10367.	1.3	70
247	Pt@CeO ₂ Multicore@Shell Self-Assembled Nanospheres: Clean Synthesis, Structure Optimization, and Catalytic Applications. Journal of the American Chemical Society, 2013, 135, 15864-15872.	6.6	323
248	One-dimensional channel-structured Eu-MOF for sensing small organic molecules and Cu2+ ion. Journal of Materials Chemistry A, 2013, 1, 11043.	5.2	341
249	Supramolecular isomerism, single-crystal to single-crystal transformation induced by release of in situ generated I2 between two supramolecular frameworks. Dalton Transactions, 2013, 42, 5619.	1.6	8
250	Microwave-assisted synthesis and down- and up-conversion luminescent properties of BaYF5:Ln (Ln =) Tj ETQq0 (ე	Overlock 10 T
251	Vapor-phase crystallization route to oxidized Cu foils in air as anode materials for lithium-ion batteries. CrystEngComm, 2013, 15, 144-151.	1.3	87

#	Article	IF	CITATIONS
253	Size-dependent catalytic properties of Au nanoparticles supported on hierarchical nickel silicate nanostructures. Dalton Transactions, 2013, 42, 7888-7893.	1.6	33
254	Synthesis of flower-like nickel oxide/nickel silicate nanocomposites and their enhanced electrochemical performance as anode materials for lithium batteries. Materials Letters, 2013, 93, 5-8.	1.3	28
255	Template-free solvothermal synthesis and enhanced thermoelectric performance of Sb2Te3 nanosheets. Journal of Alloys and Compounds, 2013, 558, 6-10.	2.8	29
256	Hydrothermal synthetic strategies of inorganic semiconducting nanostructures. Chemical Society Reviews, 2013, 42, 5714.	18.7	437
257	Efficient blueâ€emitting Ir(III) complexes with phenylâ€methylâ€benzimidazolyl and picolinate ligands: A DFT and timeâ€dependent DFT study. International Journal of Quantum Chemistry, 2013, 113, 1641-1649.	1.0	13
258	Near-infrared photoluminescent flowerlike α-In2Se3 nanostructures from a solvothermal treatment. Chemical Engineering Journal, 2013, 225, 474-480.	6.6	24
259	Homogeneous CoO on Graphene for Binderâ€Free and Ultralongâ€Life Lithium Ion Batteries. Advanced Functional Materials, 2013, 23, 4345-4353.	7.8	333
260	Two high-connected metal–organic frameworks based on d10-metal clusters: syntheses, structural topologies and luminescent properties. Dalton Transactions, 2013, 42, 8183.	1.6	32
261	Graphene Oxide Induced Formation of Pt–CeO ₂ Hybrid Nanoflowers with Tunable CeO ₂ Thickness for Catalytic Hydrolysis of Ammonia Borane. Chemistry - A European Journal, 2013, 19, 8082-8086.	1.7	50
262	CeO ₂ â€Based Pd(Pt) Nanoparticles Grafted onto Fe ₃ O ₄ /Graphene: A General Selfâ€Assembly Approach To Fabricate Highly Efficient Catalysts with Magnetic Recyclable Capability. Chemistry - A European Journal, 2013, 19, 5169-5173.	1.7	19
263	A Series of Metal–Organic Frameworks Constructed From a V-shaped Tripodal Carboxylate Ligand: Syntheses, Structures, Photoluminescent, and Magnetic Properties. Crystal Growth and Design, 2013, 13, 2756-2765.	1.4	52
264	A multifunctional proton-conducting and sensing pillar-layer framework based on [24-MC-6] heterometallic crown clusters. Chemical Communications, 2013, 49, 8483.	2.2	67
265	Luminescent character of mesoporous silica with Er2O3 composite materials. Microporous and Mesoporous Materials, 2013, 170, 113-122.	2.2	18
266	Phase-tunable synthesis and upconversion photoluminescence of rare-earth-doped sodium scandium fluoride nanocrystals. CrystEngComm, 2013, 15, 6901.	1.3	22
267	Tunnel-dependent supercapacitance of MnO ₂ : effects of crystal structure. Journal of Applied Crystallography, 2013, 46, 1128-1135.	1.9	65
268	Hopper-like framework growth evolution in a cubic system: a case study of Cu ₂ O. Journal of Applied Crystallography, 2013, 46, 1603-1609.	1.9	24
269	Density functional theory and timeâ€dependent density functional theory study on a series of iridium complexes with tetraphenylimidodiphosphinate ligand. Journal of Physical Organic Chemistry, 2013, 26, 840-848.	0.9	11
270	Hollow Zn ₂ GeO ₄ Nanorods Supported on Reduced Graphene Oxides as an Environment-Friendly High-Capacity Anode Material for Lithium Ion Batteries. Science of Advanced Materials, 2013, 5, 523-529.	0.1	9

#	Article	IF	CITATIONS
271	Hierarchical Gold Nanoflower Syntheses and Surface-Enhanced Raman Scattering Properties Research. Science of Advanced Materials, 2013, 5, 1797-1800.	0.1	1
272	Poly[[diaqua(μ-4,4′-bipyridineN,N′-dioxide-κ2O:O′)(μ-terephthalato-κ2O1:O4)cobalt(II)] 4,4′-bipyri monosolvate]. Acta Crystallographica Section E: Structure Reports Online, 2012, 68, m1307-m1307.	dineN,Nâŧ 0.2	€²-dioxide 0
273	CRYSTALLIZATION OF OXIDES AS FUNCTIONAL MATERIALS. Functional Materials Letters, 2012, 05, 1230002.	0.7	51
274	Poly[[diaquabis{μ-4-[6-(4-carboxyphenyl)-4,4′-bipyridin-2-yl]benzoato-κ2O:N4′}zinc] dimethylformamide tetrasolvate]. Acta Crystallographica Section E: Structure Reports Online, 2012, 68, m1413-m1413.	0.2	1
275	An active-site-accessible porous metal–organic framework composed of triangular building units: preparation, catalytic activity and magnetic property. Chemical Communications, 2012, 48, 11118.	2.2	69
276	New class of Preyssler-lanthanide complexes with modified and extended structures tuned by the lanthanide contraction effect. Dalton Transactions, 2012, 41, 2399.	1.6	31
277	Microwave-assisted synthesis of BiOBr/graphene nanocomposites and their enhanced photocatalytic activity. Dalton Transactions, 2012, 41, 10472.	1.6	96
278	Three unprecedented open frameworks based on a pyridyl-carboxylate: synthesis, structures and properties. CrystEngComm, 2012, 14, 1681-1686.	1.3	19
279	Facile Synthesis of Wellâ€Dispersed Silver Nanoparticles on Hierarchical Flowerâ€like Ni ₃ Si ₂ O ₅ (OH) ₄ with a High Catalytic Activity towards 4â€Nitrophenol Reduction. Chemistry - an Asian Journal, 2012, 7, 2955-2961.	1.7	15
280	Self-assembled 3D flower-like hierarchical Fe3O4/KxMnO2 core–shell architectures and their application for removal of dye pollutants. CrystEngComm, 2012, 14, 2866.	1.3	14
281	Synthesis of monodispersed Au–PbS hybrid nanocrystals via a solid–liquid interfacial reaction. CrystEngComm, 2012, 14, 7552.	1.3	2
282	Raisin-like rare earth doped gadolinium fluoride nanocrystals: microwave synthesis and magnetic and upconversion luminescent properties. CrystEngComm, 2012, 14, 4266.	1.3	29
283	Co2GeO4 nanoplates and nano-octahedrons from low-temperature controlled synthesis and their magnetic properties. CrystEngComm, 2012, 14, 7306.	1.3	12
284	Water-soluble Au–CeO2 hybrid nanosheets with high catalytic activity and recyclability. Dalton Transactions, 2012, 41, 7193.	1.6	22
285	Bi2Te3 nanoplates and nanoflowers: Synthesized by hydrothermal process and their enhanced thermoelectric properties. CrystEngComm, 2012, 14, 2159.	1.3	125
286	Facile synthesis of Pt3Sn/graphene nanocomposites and their catalysis for electro-oxidation of methanol. CrystEngComm, 2012, 14, 7137.	1.3	14
287	Synthesis of highly active Pt–CeO2 hybrids with tunable secondary nanostructures for the catalytic hydrolysis of ammonia borane. Chemical Communications, 2012, 48, 10207.	2.2	104
288	Spin canting magnetization in a 3D Cu(ii) complex based on molybdate oxide cluster and 5-triazole isophthalic acid. Dalton Transactions, 2012, 41, 13267.	1.6	19

#	Article	IF	CITATIONS
289	Green and controlled synthesis of Cu2O–graphene hierarchical nanohybrids as high-performance anode materials for lithium-ion batteries via an ultrasound assisted approach. Dalton Transactions, 2012, 41, 4316.	1.6	64
290	Syntheses, structures, photoluminescence, and magnetic properties of (3,6)- and 4-connected lanthanide metal–organic frameworks with a semirigid tricarboxylate ligand. Dalton Transactions, 2012, 41, 4772.	1.6	47
291	Green synthesis of Pt/CeO2/graphene hybrid nanomaterials with remarkably enhanced electrocatalytic properties. Chemical Communications, 2012, 48, 2885.	2.2	131
292	Rhodium–nickel nanoparticles grown on graphene as highly efficient catalyst for complete decomposition of hydrous hydrazine at room temperature for chemical hydrogen storage. Energy and Environmental Science, 2012, 5, 6885.	15.6	214
293	Lanthanide Anionic Metal–Organic Frameworks Containing Semirigid Tetracarboxylate Ligands: Structure, Photoluminescence, and Magnetism. Crystal Growth and Design, 2012, 12, 1808-1815.	1.4	100
294	Syntheses, Structures, and Photoluminescent Properties of Coordination Polymers Based on 1,4-Bis(imidazol-l-yl-methyl)benzene and Various Aromatic Dicarboxylic Acids. Crystal Growth and Design, 2012, 12, 253-263.	1.4	84
295	Crystallization design of MnO2 towards better supercapacitance. CrystEngComm, 2012, 14, 5892.	1.3	187
296	Comparative Study of Structural Changes in NH ₃ BH ₃ , LiNH ₂ BH ₃ , and KNH ₂ BH ₃ During Dehydrogenation Process. Journal of Physical Chemistry C, 2012, 116, 5957-5964.	1.5	57
297	A series of POM/Ag-based hybrids: distinct forms and assembly of [AgxLy] complexes through combinational effects of POM and isomeric ligands. CrystEngComm, 2012, 14, 6452.	1.3	34
298	Highly transparent bulk PMMA/ZnO nanocomposites with bright visible luminescence and efficient UV-shielding capability. Journal of Materials Chemistry, 2012, 22, 11971.	6.7	70
299	Syntheses, structures and physical properties of transition metal–organic frameworks assembled from trigonal heterofunctional ligands. Dalton Transactions, 2012, 41, 10412.	1.6	58
300	Syntheses, Structures, and Photoluminescent Properties of 12 New Metal–Organic Frameworks Constructed by a Flexible Dicarboxylate and Various N-Donor Ligands. Crystal Growth and Design, 2012, 12, 2397-2410.	1.4	129
301	Synthesis of high-quality l–Ill–VI semiconductor supported Au particles and their catalytic performance. Catalysis Science and Technology, 2012, 2, 488.	2.1	12
302	Selectively Deposited Noble Metal Nanoparticles on Fe ₃ O ₄ /Graphene Composites: Stable, Recyclable, and Magnetically Separable Catalysts. Chemistry - A European Journal, 2012, 18, 7601-7607.	1.7	126
303	Microwaveâ€Assisted Modular Fabrication of Nanoscale Luminescent Metalâ€Organic Framework for Molecular Sensing. ChemPhysChem, 2012, 13, 2734-2738.	1.0	67
304	An unusual three-dimensional self-penetrating network derived from cross-linking of two-fold interpenetrating nets via ligand-unsupported Ag–Ag bonds: synthesis, structure, luminescence, and theoretical study. New Journal of Chemistry, 2012, 36, 877.	1.4	25
305	Lithium hydrazide as a potential compound for hydrogen storage. International Journal of Hydrogen Energy, 2012, 37, 5750-5753.	3.8	6
306	Synthesis of Fe3O4 nanoflowers by a simple and novel solvothermal process. Materials Letters, 2012, 76, 90-92.	1.3	12

#	Article	IF	CITATIONS
307	Selective crystallization with preferred lithium-ion storage capability of inorganic materials. Nanoscale Research Letters, 2012, 7, 149.	3.1	32
308	Folded Structured Graphene Paper for High Performance Electrode Materials. Advanced Materials, 2012, 24, 1089-1094.	11.1	619
309	Some Strategies for Improving the Photocatalytic Efficiency of Semiconductor Photocatalyst. Reviews in Advanced Sciences and Engineering, 2012, 1, 165-172.	0.6	4
310	Efficient White Electroluminescent Device with Stable Emission Spectrum. Acta Chimica Sinica, 2012, 70, 1904.	0.5	0
311	Research progresses of lanthanide sulfides. Scientia Sinica Chimica, 2012, 42, 1337-1355.	0.2	1
312	Solid state NMR study on the thermal decomposition pathway of sodium amidoborane NaNH2BH3. Journal of Materials Chemistry, 2011, 21, 2609.	6.7	48
313	Rhombic dodecahedral Fe3O4: ionic liquid-modulated and microwave-assisted synthesis and their magnetic properties. CrystEngComm, 2011, 13, 6017.	1.3	41
314	Fabrication of fluorescent silica–Au hybrid nanostructures for targeted imaging of tumor cells. Dalton Transactions, 2011, 40, 4800.	1.6	15
315	Five three/two-fold interpenetrating architectures from self-assembly of fluorene-2,7-dicarboxylic acid derivatives and d10 metals. CrystEngComm, 2011, 13, 2935.	1.3	33
316	Surfactant-free preparation of NiO nanoflowers and their lithium storage properties. CrystEngComm, 2011, 13, 4903.	1.3	34
317	Cobalt and nickel with various morphologies: mineralizer-assisted synthesis, formation mechanism, and magnetic properties. CrystEngComm, 2011, 13, 223-229.	1.3	15
318	Three three-dimensional anionic metal–organic frameworks with (4,8)-connected alb topology constructed from a semi-rigid ligand and polynuclear metal clusters. CrystEngComm, 2011, 13, 6057.	1.3	19
319	Hierarchically structured Fe ₃ O ₄ microspheres: morphology control and their application in wastewater treatment. CrystEngComm, 2011, 13, 642-648.	1.3	80
320	Synthesis of 3D Hierarchical Fe ₃ O ₄ /Graphene Composites with High Lithium Storage Capacity and for Controlled Drug Delivery. Journal of Physical Chemistry C, 2011, 115, 21567-21573.	1.5	288
321	Syntheses, Structures, Photoluminescence, and Gas Adsorption of Rare Earth–Organic Frameworks Based on a Flexible Tricarboxylate. Crystal Growth and Design, 2011, 11, 5469-5474.	1.4	41
322	Rare-Earth-Doped Bifunctional Alkaline-Earth Metal Fluoride Nanocrystals via a Facile Microwave-Assisted Process. Inorganic Chemistry, 2011, 50, 5327-5329.	1.9	12
323	Porous Co3O4 microcubes: hydrothermal synthesis, catalytic and magnetic properties. CrystEngComm, 2011, 13, 2123.	1.3	60
324	Microwave-assisted synthesis of hydrophilic BaYF ₅ :Tb/Ce,Tb green fluorescent colloid nanocrystals. Dalton Transactions, 2011, 40, 142-145.	1.6	28

#	Article	IF	CITATIONS
325	Well-defined Sb2S3 microspheres: High-yield synthesis, characterization, their optical and electrochemical hydrogen storage properties. Solid State Sciences, 2011, 13, 1226-1231.	1.5	10
326	Morphology-controlled synthesis of $\hat{l}\pm$ -Fe2O3 nanostructures with magnetic property and excellent electrocatalytic activity for H2O2. Solid State Sciences, 2011, 13, 2129-2136.	1.5	7
327	Superior electrode performance of mesoporous hollow TiO2 microspheres through efficient hierarchical nanostructures. Journal of Power Sources, 2011, 196, 8618-8624.	4.0	52
328	Synthesis of Ferrite Nanocrystals Stabilized by Ionicâ€Liquid Molecules through a Thermal Decomposition Route. Chemistry - A European Journal, 2011, 17, 920-924.	1.7	8
329	Synthesis and luminescent properties of organic–inorganic hybrid macroporous materials doped with lanthanide (Eu/Tb) complexes. Optical Materials, 2011, 33, 582-585.	1.7	18
330	Direct hydrothermal synthesis of single-crystalline triangular Fe3O4 nanoprisms. CrystEngComm, 2010, 12, 2060.	1.3	68
331	Guests inducing p-sulfonatocalix[4]arenes into nanocapsule and layer structure. Journal of Solid State Chemistry, 2010, 183, 1457-1463.	1.4	15
332	Uniform In2S3 octahedron-built microspheres: Bioinspired synthesis andÂoptical properties. Solid State Sciences, 2010, 12, 39-44.	1.5	12
333	Synthesis and Optical Properties of Europium omplexâ€Doped Inorganic/Organic Hybrid Materials Built from Oxo–Hydroxo Organotin Nano Building Blocks. Chemistry - A European Journal, 2010, 16, 1903-1910.	1.7	67
334	Colloidal Nobleâ€Metal and Bimetallic Alloy Nanocrystals: A General Synthetic Method and Their Catalytic Hydrogenation Properties. Chemistry - A European Journal, 2010, 16, 6251-6256.	1.7	36
335	Thermal decomposition of alkaline-earth metal hydride and ammonia borane composites. International Journal of Hydrogen Energy, 2010, 35, 12405-12409.	3.8	45
336	Bioinspired Green Synthesis of Nanomaterials and their Applications. Current Nanoscience, 2010, 6, 452-468.	0.7	12
337	Hydrothermal synthesis and upconversion photoluminescence properties of lanthanide doped YF3 sub-microflowers. CrystEngComm, 2010, 12, 3537.	1.3	31
338	Controllable Synthesis of NIR-Luminescent ErQ3Nano-/Microstructures through Self-assembly Growth. Crystal Growth and Design, 2010, 10, 4662-4667.	1.4	14
339	Lanthanide doped Y6O5F8/YF3 microcrystals: phase-tunable synthesis and bright white upconversion photoluminescence properties. Dalton Transactions, 2010, 39, 9153.	1.6	40
340	High-Brightness, Broad-Spectrum White Organic Electroluminescent Device Obtained by Designing Light-Emitting Layers as also Carrier Transport Layers. Journal of Physical Chemistry C, 2010, 114, 21723-21727.	1.5	17
341	Room temperature, template-free synthesis of BiOI hierarchical structures: Visible-light photocatalytic and electrochemical hydrogen storage properties. Dalton Transactions, 2010, 39, 3273.	1.6	169
342	Novel Multifunctional Nanocomposites: Magnetic Mesoporous Silica Nanospheres Covalently Bonded with Near-Infrared Luminescent Lanthanide Complexes. Langmuir, 2010, 26, 3596-3600.	1.6	78

#	Article	IF	CITATIONS
343	Activation of Ammonia Borane Hybridized with Alkalineâ^'Metal Hydrides: A Low-Temperature and High-Purity Hydrogen Generation Material. Journal of Physical Chemistry C, 2010, 114, 14662-14664.	1.5	33
344	Near-infrared luminescent copolymerized hybrid materials built from tin nanoclusters and PMMA. Nanoscale, 2010, 2, 2096.	2.8	35
345	Tetracarboxylate-based Co(ii), Ni(ii) and Cu(ii) three-dimensional coordination polymers: syntheses, structures and magnetic properties. Dalton Transactions, 2010, 39, 9123.	1.6	41
346	Fabrication and characterization of magnetic mesoporous silica nanospheres covalently bonded with europium complex. Dalton Transactions, 2010, 39, 5166.	1.6	15
347	One-pot synthesis of flowerlike Ni7S6and its application in selective hydrogenation of chloronitrobenzene. Journal of Materials Chemistry, 2010, 20, 1078-1085.	6.7	75
348	Cubic spinel In4SnS8: electrical transport properties and electrochemical hydrogen storage properties. Dalton Transactions, 2010, 39, 7021.	1.6	13
349	Synthesis, structure and characterization of new 1D and 2D Ni(II) coordination polymers. Solid State Sciences, 2009, 11, 364-367.	1.5	4
350	Carbon anode material formed from template molecules occluded in a magnesium-substituted aluminophosphate. Materials Chemistry and Physics, 2009, 113, 309-313.	2.0	2
351	Fabrication and characterization of uniform Fe3O4 octahedral micro-crystals. Materials Letters, 2009, 63, 307-309.	1.3	28
352	Near-infrared luminescent mesoporous MCM-41 materials covalently bonded with ternary thulium complexes. Microporous and Mesoporous Materials, 2009, 117, 278-284.	2.2	29
353	Synthesis, characterization, and near-infrared luminescent properties of the ternary thulium complex covalently bonded to mesoporous MCM-41. Journal of Solid State Chemistry, 2009, 182, 435-441.	1.4	22
354	Facile Synthesis and Assemblies of Flowerlike SnS ₂ and In ³⁺ -Doped SnS ₂ : Hierarchical Structures and Their Enhanced Photocatalytic Property. Journal of Physical Chemistry C, 2009, 113, 1280-1285.	1.5	201
355	Surface photovoltage characterization of a ZnO nanowire array/CdS quantum dot heterogeneous film and its application for photovoltaic devices. Nanotechnology, 2009, 20, 155707.	1.3	110
356	Molecular Nanocluster with a [Sn4Ga4Zn2Se20]8â^' T3 Supertetrahedral Core. Inorganic Chemistry, 2009, 48, 4628-4630.	1.9	41
357	Hydrothermal Synthesis, Structures, and Luminescent Properties of Seven d10 Metalâ^'Organic Frameworks Based on 9,9-Dipropylfluorene-2,7-Dicarboxylic Acid (H2DFDA). Crystal Growth and Design, 2009, 9, 1394-1401.	1.4	101
358	Stabilization of Imidosamarium(III) Cubane by Amidinates. Inorganic Chemistry, 2009, 48, 6344-6346.	1.9	47
359	Self-Assembled Growth of AgIn(MoO4)2 Submicroplates into Hierarchical Structures and Their Near-Infrared Luminescent Properties. Crystal Growth and Design, 2009, 9, 848-852.	1.4	22
360	3D Fe3S4 flower-like microspheres: high-yield synthesis via a biomolecule-assisted solution approach, their electrical, magnetic and electrochemical hydrogen storage properties. Dalton Transactions, 2009, , 9246.	1.6	102

#	Article	IF	CITATIONS
361	A study on the near-infrared luminescent properties of xerogel materials doped with dysprosium complexes. Dalton Transactions, 2009, , 6593.	1.6	53
362	Synthesis, characterization and optical property of flower-like indium tin sulfide nanostructures. Dalton Transactions, 2009, , 1620.	1.6	19
363	Culn(WO4)2 nanospindles and nanorods: controlled synthesis and host for lanthanide near-infrared luminescence properties. CrystEngComm, 2009, 11, 1987.	1.3	14
364	Synthesis, characterization and assembly of BiOCl nanostructure and their photocatalytic properties. CrystEngComm, 2009, 11, 1857.	1.3	210
365	Near-infrared luminescent xerogel materials covalently bonded with ternary lanthanide [Er(iii), Nd(iii), Yb(iii), Sm(iii)] complexes. Dalton Transactions, 2009, , 2406.	1.6	57
366	Selfâ€Assembly of <i>p</i> â€Sulfonatocalix[4]arene and a Ag–hmt Coordination Polymer into a Porous Structure. European Journal of Inorganic Chemistry, 2008, 2008, 1756-1759.	1.0	19
367	Erbium omplexâ€Doped Nearâ€Infrared Luminescent and Magnetic Macroporous Materials. European Journal of Inorganic Chemistry, 2008, 2008, 5513-5518.	1.0	12
368	Rectangular AgIn(WO ₄) ₂ Nanotubes: A Promising Photoelectric Material. Advanced Functional Materials, 2008, 18, 2328-2334.	7.8	88
369	Hydrothermal Synthesis and Thermoelectric Transport Properties of Impurityâ€Free Antimony Telluride Hexagonal Nanoplates. Advanced Materials, 2008, 20, 1892-1897.	11.1	162
370	Design and synthesis of near-IR luminescent mesoporous materials covalently linked with tris(8-hydroxyquinolinate)lanthanide(III) complexes. Microporous and Mesoporous Materials, 2008, 115, 535-540.	2.2	28
371	Studies on the magnetism of cobalt ferrite nanocrystals synthesized by hydrothermal method. Journal of Solid State Chemistry, 2008, 181, 245-252.	1.4	260
372	Ternary lanthanide (Er3+, Nd3+, Yb3+, Sm3+, Pr3+) complex-functionalized mesoporous SBA-15 materials that emit in the near-infrared range. Journal of Photochemistry and Photobiology A: Chemistry, 2008, 199, 57-63.	2.0	24
373	Syntheses, crystal structures, visible and near-IR luminescent properties of ternary lanthanide (Dy3+,) Tj ETQq1 1 of Luminescence, 2008, 128, 1957-1964.	0.784314 1.5	4 rgBT /Over 57
374	Preparation and gas storage of high surface area microporous carbon derived from biomass source cornstalks. Bioresource Technology, 2008, 99, 4803-4808.	4.8	76
375	Syntheses, crystal structures and near-infrared luminescent properties of holmium (Ho) and praseodymium (Pr) ternary complexes. Inorganic Chemistry Communication, 2008, 11, 531-534.	1.8	36
376	Hydrothermal Synthesis and High Photocatalytic Activity of 3D Wurtzite ZnSe Hierarchical Nanostructures. Journal of Physical Chemistry C, 2008, 112, 17095-17101.	1.5	115
377	Morphology-Controlled Synthesis of Magnetites with Nanoporous Structures and Excellent Magnetic Properties. Chemistry of Materials, 2008, 20, 198-204.	3.2	152
378	Constructing channel structures based on the assembly of p-sulfonatocalix[4]arene nanocapsules and [M(bpdo)3]2+(M = Cu, Zn). Chemical Communications, 2008, , 4918.	2.2	24

#	Article	IF	CITATIONS
379	Microemulsion-mediated solvothermal synthesis and photoluminescent property of 3D flowerlike MnWO4 micro/nanocomposite structure. Solid State Sciences, 2008, 10, 1299-1304.	1.5	46
380	Self-assembly of guest-induced calix[4]arene nanocapsules into three-dimensional molecular architecture. CrystEngComm, 2008, 10, 658.	1.3	12
381	Synthesis, structures and photoluminescence of two Er(III) coordination polymers. Journal of Coordination Chemistry, 2008, 61, 945-955.	0.8	13
382	Synthesis and characterization of 1D Co/CoFe2O4 composites with tunable morphologies. Chemical Communications, 2008, , 3570.	2.2	14
383	Hydrothermal synthesis and photoluminescent properties of stacked indium sulfide superstructures. Chemical Communications, 2008, , 1476.	2.2	53
384	Facile Synthesis and Optical Property of Porous Tin Oxide and Europium-Doped Tin Oxide Nanorods through Thermal Decomposition of the Organotin. Journal of Physical Chemistry C, 2008, 112, 19939-19944.	1.5	16
385	Hydrothermal Synthesis and Characterization of Alkaline-Earth Metal Phenylphosphonate Nanostructures. Crystal Growth and Design, 2007, 7, 895-899.	1.4	17
386	Structural Study of Silver(I) Sulfonate Complexes with Pyrazine Derivatives. Inorganic Chemistry, 2007, 46, 7299-7311.	1.9	65
387	Effect of silver nanoparticles on luminescent properties of europium complex in di-ureasil hybrid materials. Journal of Luminescence, 2007, 122-123, 892-895.	1.5	3
388	Intrinsic peroxidase-like activity of ferromagnetic nanoparticles. Nature Nanotechnology, 2007, 2, 577-583.	15.6	5,080
389	Microporous carbon derived from pinecone hull as anode material for lithium secondary batteries. Materials Letters, 2007, 61, 5209-5212.	1.3	50
390	Syntheses, Structures, and Characterizations of Four New Silver(I) Sulfonate Coordination Polymers with Neutral Ligands. Crystal Growth and Design, 2006, 6, 209-215.	1.4	99
391	Systematic Synthesis and Characterization of Single-Crystal Lanthanide Phenylphosphonate Nanorods. Inorganic Chemistry, 2006, 45, 1201-1207.	1.9	37
392	Selected-Control Synthesis of Metal Phosphonate Nanoparticles and Nanorods. Inorganic Chemistry, 2005, 44, 2140-2142.	1.9	48
393	Influence of Neutral Ligands on the Structures of Silver(I) Sulfonates. Inorganic Chemistry, 2005, 44, 9374-9383.	1.9	151
394	Two Coordination Polymers of Ag(I) with 5-Sulfosalicylic Acid. Crystal Growth and Design, 2005, 5, 807-812.	1.4	155
395	Formation of nanographite using GaPO ₄ ‣TA as template. Chinese Journal of Chemistry, 2004, 22, 1399-1402.	2.6	0
396	Protective Coating of Superparamagnetic Iron Oxide Nanoparticles. Chemistry of Materials, 2003, 15, 1617-1627.	3.2	450

#	Article	IF	CITATIONS
397	Superior Oxygen Evolution Reaction Performance of Co ₃ O ₄ /NiCo ₂ O ₄ /Ni Foam Composite with Hierarchical Structure. ACS Sustainable Chemistry and Engineering, 0, , .	3.2	7